Photolysis and oxidation by OH radicals of two carbonyl nitrates: 4-nitrooxy-2-butanone and 5-nitrooxy-2-pentanone

Bénédicte Picquet-Varrault[1], Ricardo Suarez-Bertoa[2], Marius Duncianu[3], Mathieu Cazaunau[1], Edouard Pangui[1], Marc David[1], Jean-François Doussin[1]

[1] LISA, UMR CNRS 7583, Université Paris-Est Créteil, Université de Paris, Institut Pierre Simon Laplace (IPSL), Créteil, France

[2] European Commission Joint Research Centre (JRC), Ispra, Italy

[3] System Analyst Interscience BV, Brussels, Belgium

Correspondence to: B. Picquet-Varrault (benedicte.picquet-varrault@lisa.u-pec.fr)

Abstract

Multifunctional organic nitrates, including carbonyl nitrates, are important species formed in NOx rich atmospheres by the degradation of VOCs. These compounds have been shown to play a key role in the transport of reactive nitrogen and consequently in the ozone budget, but also to be important components of the total organic aerosol. However, very little is known about their reactivity in both gas and condensed phases. Following a previous study we published on the gas-phase reactivity of α-nitrooxy ketones, the photolysis and the reaction with OH radicals of 4-nitrooxy-2-butanone and 5-nitrooxy-2-pentanone, respectively a β-nitrooxy ketone and a γ-nitrooxy ketone, were investigated for the first time in simulation chambers. Ambient photolysis frequencies calculated for 40° latitude North (1st July, noon) were found to be $(6.1 \pm 0.9) \times 10^{-5}$ s^{-1} and $(3.3 \pm 0.9) \times 10^{-5}$ s^{-1} for 4-nitrooxy-2-butanone and 5-nitrooxy-2-pentanone, respectively. These results demonstrate that photolysis is a very efficient sink for these compounds with atmospheric lifetimes of few hours. It was also concluded that, similarly to α-nitrooxy ketones, β-nitrooxy ketones have enhanced UV absorption cross sections and quantum yields equal or close to unity. They also suggest that γ-nitrooxy ketones have lower enhancement of cross sections which can easily be explained by the larger distance between the two chromophore groups. Thanks to a product study, branching ratio between the two possible photodissociation pathways are also proposed. Rate constants for the reaction with OH radicals were found to be $(2.9 \pm 1.0) \times 10^{-12}$ cm^3 molecule^{-1} s^{-1} and $(3.3 \pm 0.9) \times 10^{-12}$ cm^3 molecule^{-1} s^{-1}, respectively. These experimental data are in good agreement with rate constants estimated by the SAR of Kwok and Atkinson (1995) when using the parametrization proposed by Suarez-Bertoa et al. (2012) for carbonyl nitrates. Comparison with photolysis rates suggests that OH-initiated oxidation of carbonyl nitrates is a less efficient sink than photodissociation but is not negligible in polluted area.

1 Introduction

1

Organic nitrates (ONs) play an important role as sinks or temporary reservoirs of NOx, as well as on ozone production in the atmosphere (Perring et al., 2013; Perring et al., 2010; Ito et al., 2007). They are formed by the degradation of VOCs in presence of NOx through two main processes: i) the reaction of peroxy radical, produced by the oxidation of VOCs, with NO. The major pathway is generally the reaction (1a) that leads to NO_2 formation. The reaction (1b) is a minor channel but it becomes gradually more important with increasing peroxy radical carbon chain length (Atkinson and Arey, 2003; Finlayson-Pitts and Pitts, 2000).

$$RO_2 + NO \rightarrow RO + NO_2 \qquad\qquad (1a)$$

$$RO_2 + NO \rightarrow RONO_2 \qquad\qquad (1b)$$

ii) The reaction of unsaturated VOCs with NO_3 radical, which proceeds mainly by addition of the nitrate radical on the double bond to produce nitro-alkyl radicals that can evolve into organic nitrates.

Among the organic nitrates, a variety of multifunctional species such as hydroxy-nitrates, carbonyl-nitrates and dinitrates are formed. The formed species have been shown to significantly contribute to the nitrogen budget in both rural and urban areas (Perring et al. 2013). Beaver et al. (2012) have observed that carbonyl nitrates, formed as second generation nitrates from isoprene, are an important fraction of the total organic nitrates observed over Sierra Nevada in summer. These observations are supported by several studies that investigated the photooxidation of isoprene in simulation chambers (Paulot et al., 2009, Müller et al., 2014). These multifunctional organic nitrates are also semi-/non-volatile and highly soluble species and are thus capable of partitioning into the atmospheric condensed phases (droplets, aerosols). Numerous field observations of the chemical composition of atmospheric particles have shown that organic nitrates represent a significant fraction (up to 75% in mass) of the total organic aerosol (OA) demonstrating that these species are important components of total OA (Ng et al., 2017).

Several modeling studies have also confirmed that multifunctional organic nitrates, in particular isoprene nitrates, play a key role in the transport of reactive nitrogen and consequently in the formation of ozone and other secondary pollutants at the regional and global scales (Horowitz et al., 2007; Mao et al., 2013; Squire et al., 2015). In particular, Mao et al. (2013) have performed simulations based on data from the ICARTT aircraft campaign across the eastern U.S. in 2004. They have shown that ONs, which are mainly composed of secondary organic nitrates, including a large fraction of carbonyl nitrates, provide an important pathway for exporting NOx from the U.S.'s boundary layer, even exceeding the export of PANs. However, these modeling studies also point out the need for additional experimental data to better describe the sinks in both gas and condensed phases of multifunctional organic nitrates in models.

Recent experimental studies have revealed that hydrolysis in aerosol phase may be a very efficient sink of organic nitrates in the atmosphere (Bean and Hildebrand Ruiz, 2015; Rindelaub et al., 2015). These works also suggest that the rate of these reactions strongly depends on the organic nitrate chemical structure and that additional work is needed to better understand these processes. In the gas-phase, photolysis and reaction with OH radical are expected to dominate the fate of organic nitrates (Roberts et al., 1990; Turberg et al., 1990). In a previous study, we have measured the photolysis frequencies and the rate constants for the OH-oxidation of 3 carbonyl nitrates (α-nitrooxyacetone, 3-nitrooxy-2-butanone, and 3-methyl-3-nitrooxy-2-butanone) and we have shown that photolysis is the dominant sink for these compounds (Suarez-Bertoa et al., 2012). By comparison

with absorption cross sections provided by Barnes et al. (1993), Müller et al. (2014) suggested i) that the α-nitrooxy ketones have enhanced absorption cross sections, due to the interaction between the –C=O and the -ONO$_2$ chromophore groups and ii) that the photolysis quantum yield is close to unity and O–NO$_2$ dissociation is the likely major channel. They also showed that this enhancement was larger at the higher wavelengths, where the absorption by the nitrate chromophore is very small. Therefore, they concluded that the absorption by the carbonyl chromophore was the one enhanced due to the neighbouring nitrate group.

These results are significant as they demonstrate that photolysis rates of these multifunctional species cannot be calculated as the sum of the monofunctional species (ketone + alkyl nitrate) ones. However, only α-nitrooxy ketones were studied in those works which leaves open the question of the persistence of the enhancement effect when the distance between the two functional groups increases. More recently, Xiong et al. (2016) have studied the photochemical degradation (photolysis, OH-oxidation and ozonolysis) of *trans*-2-methyl-4-nitrooxy-2-buten-1-al (also called 4,1-isoprene nitrooxy enal) in order to better assess – as a model compound - the reactivity of carbonyl nitrates formed by the NO$_3$-initiated oxidation of isoprene. This compound has a conjugated chromophore –C=C-C=O in β position of the nitrate group. The authors measured the absorption cross sections of the nitroxy enal and compared them to those for the monofunctional species, i.e. methacrolein and isopropyl nitrate. They concluded that molecules containing β-nitrooxy ketones functionalities have also enhanced UV absorption cross sections. They also studied the kinetic and mechanisms for the oxidation of the nitroxy enal by OH and O$_3$ and showed that the reaction with OH radicals is fairly fast. Photolysis and reaction with OH are thus the two main loss processes of *trans*-2-methyl-4-nitrooxy-2-buten-1-al, leading to a tropospheric lifetime of less than 1 h.

Given the large contribution of the carbonyl nitrates to the organic nitrate pool and the importance of their photochemistry for the NOx budget, we present a study that aims at providing new experimental data on the gas-phase reactivity of these compounds. The study also seeks to disclose how photolysis and reaction with OH radical of carbonyl nitrates are affected by modifying their carbon chain length and the position of the two functional groups present in their molecular structure. Here, we provide the first photolysis frequencies and also the first rate constants for the OH-oxidation of two carbonyl nitrates: 4-nitrooxy-2-butanone and 5-nitrooxy-2-pentanone.

2 Experimental section

2.1 Reactants syntheses

As a usual OH precursor in simulation chamber experiments, isopropyl nitrite was synthesized by dropwise addition of a dilute solution of H$_2$SO$_4$ into a mixture of NaNO$_2$ and isopropanol following the classical protocol proposed by Taylor et al. (1980).

On the contrary, 4-nitrooxy-2-butanone and 5-nitrooxy-2-pentanone were synthesized for the first time. A great care was taken to the development of a robust process: 4-nitrooxy-2-butanone and 5-nitrooxy-2-pentanone syntheses are based on Kames' method (Kames et al., 1993). This method consists in a liquid/gas phase reaction where the corresponding hydroxy-ketone reacts with NO$_3$ radicals released from the dissociation of N$_2$O$_5$. N$_2$O$_5$

was preliminarily synthesized in a vacuum line by reaction of NO_2 with ozone, as described by Scarfogliero et al. (2006). The synthesis of the carbonyl nitrate is performed in a dedicated vacuum line connected to two bulbs, one containing the hydroxy-ketone, the other one containing N_2O_5. The two bulbs are also connected to each other. In a first step, the bulbs are placed in a liquid N_2 cryogenic trap and pumped in order to remove air and impurities. In a second step, the cryogenic trap is removed from the bulb containing N_2O_5 in order to let it warm and transfer into the bulb containing the hydroxy-ketone. Then, the bulb containing both reactants is stirred and kept at ice temperature for approximatively 1h. Finally, the resulting carbonyl nitrate and nitric acid, its co-product, were separated by liquid-liquid extraction using dichloromethane and water. The carbonyl nitrate structure and purity were verified by FT-IR and GC-MS. Traces of impurities (HCOOH and CH_3COOH) have been detected. The carbonyl nitrates were stored at -18° C and under nitrogen atmosphere to prevent them from decomposition. Infrared spectra of 4-nitroxy-2-butanone and 5-nitroxy-2-pentanone are available on EUROCHAMP Data Centre (https://data.eurochamp.org).

2.2 Determination of photolysis frequencies

The photolysis frequencies of the two carbonyl nitrates were determined by carrying out experiments in the CESAM simulation chamber which is only briefly described here as detailed information can be found in Wang et al. (2011). The chamber consists of a 4.2 m^3 stainless steel vessel equipped with a multiple reflection optical system interfaced to a FTIR spectrometer (Bruker Tensor 37) and also with NO, NO_2 and O_3 analyzers (Horiba) to monitor the composition of the gas phase. The chamber is also equipped with three high pressure xenon arc lamps (MH-Diffusion, MacBeam 4000) which are combined with 7 mm Pyrex filters. This irradiation device provides a very realistic actinic flux (in comparison to the solar one, see Figure S1) which allows measuring photolysis frequencies under realistic conditions (Wang et al., 2011; Suarez-Bertoa et al., 2012). The intensity of the actinic flux was determined by measuring the photolysis rate of NO_2 (J_{NO2}) during dedicated experiments. Hence, 400 ppbv of NO_2 in 1000 mbar of N_2 were injected into CESAM chamber and kept in the dark for 20 min. The lights were then turned on during 20 min, and finally the mixture was left in the dark for an additional 20 min period. The photolysis frequency was subsequently determined using a kinetic numeric model developed for previous NOx photo-oxidation experiments in CESAM (Wang et al., 2011). The fitting of modeled values from the measured data provided a NO_2 photolysis frequency equal to 2.2×10^{-3} s^{-1} (± 0.01, 2σ error). Since the J_{NO2} on July 1 at noon at 40° latitude North (overhead ozone column 300, albedo 0.1; TUV NCAR Model, http://www.cprm.acd.ucar.edu/Models/TUV/Interactive_TUV/) is estimated to be equal to 1.03×10^{-2} s^{-1} and considering how close from the real sunlight is the irradiation light in CESAM, we assumed that a proportionality factor of 4.7 can be directly applied.

During a typical experiment, carbonyl nitrates were introduced into the chamber which was preliminarily filled at atmospheric pressure with N_2/O_2 (80/20). For the injection, the bulb containing the carbonyl nitrate was connected to the chamber and slightly heated while it was flushed with N_2. Mixing ratios of carbonyl nitrates ranged from hundreds ppb to ppm. Because carbonyl nitrates may decompose during the injection, large amounts of NO_2 (hundreds ppb) were present in the mixture. Cyclohexane was also added to the mixture as an OH-scavenger with mixing ratios of approx. 4 ppm. Considering the fact that cyclohexane is approximatively twice more reactive with OH radicals than the ketonitrates (see Results section), it was estimated that between 80 and 98% of the OH radicals were scavenged (depending on the experiment considered). The mixture was kept under

148   dark conditions during two hours to be able to assess the impact of the reactor's walls and to minimize their effects by passivation. Then, the mixture was irradiated during 3 hours. For most experiments, the mixture was

150   finally left in the dark for approximately 1 hour after the irradiation period to allow for verifying if wall losses were constant during the entire duration of the experiment.

152   During the experiment, the carbonyl nitrate loss processes can be described as:

nitrate (walls) $\rightarrow$ products   (k)   (2a)

154   nitrate + hν $\rightarrow$ products   (J)   (2b)
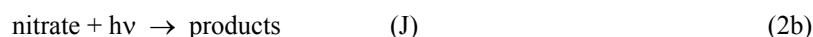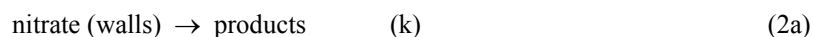
$$-\frac{d[nitrate]}{dt} = (J + k) \times [nitrate] \qquad\qquad\qquad\qquad \text{(Eq. 1)}$$

156     $$ln[nitrate]_t = ln[nitrate]_0 - (k + J) \times t \qquad\qquad\qquad\qquad \text{(Eq. 2)}$$

The reaction (2a) had to be added to the system to take into account the interaction or adsorption of the carbonyl

158   nitrates on the stainless steel walls of CESAM during the experiments. By plotting $ln[nitrate]_t$ *vs*. time, where $[nitrate]_t$ is the concentration of the carbonyl nitrate at time t, a straight line is obtained with a slope of $(k + J)$.

160   The same approach was applied to each of the 'dark' periods, before and after irradiation, to determine their respective nitrate decay rates, namely k_{before} and k_{after} and k was calculated as the average of k_{before} and k_{after} for

162   each experiment. Finally, J was calculated as the difference between the loss rate during the irradiation period (k + J) and the averaged loss rate during the dark periods (k).

164   The uncertainties were calculated by adding the respective statistical errors (2σ) associated to the dark and light periods, the former set as the average of the uncertainties determined for both dark periods (i.e., before and after

166   irradiation). However, for some experiments, it was observed that the dark decay rate before irradiation was significantly higher than the one after, suggesting that wall loss process is more complex than a "simple" first

168   order process and may decrease with time due to a passivation of the walls. More generally, interactions of gases with walls remain poorly understood and are currently subject to intensive investigations by the scientific

170   community. Here, in order to determine wall loss decays which are as representative as possible of the one during the irradiation period, the first experimental points (after the injection of the carbonyl nitrate) were not

172   taken into account for the linear fit leading to the determination of k_{before}. In addition, the uncertainty was not calculated using the approach detailed above, the statistical error being too low compared to the difference

174   between k_{before} and k_{after}. The uncertainty was thus estimated in order to include the lowest and the highest J values calculated with the highest and the lowest k value, respectively. Finally, the overall uncertainty associated

176   with the photolysis rate of each of the carbonyl nitrates was calculated as the average of the uncertainties obtained for each experiment, divided by the square root of the number of experiments (2 or 3).

178   **2.3 Determination of the OH-oxidation rate constants**

The kinetic experiments for the OH-oxidation of the carbonyl nitrates were performed in the CSA chamber at

180   room temperature and atmospheric pressure, in a mixture of N_2/O_2 (80/20). The chamber consists of a 977 L Pyrex[TM] vessel irradiated by two sets of 40 fluorescent tubes (Philips TL05 and TL03) that surround the

182   chamber. The emissions of these black lamps are centered on 360 and 420 nm, respectively. The chamber is

equipped with a multiple reflection optical system with a path length of 180 m interfaced to a FTIR spectrometer
184   (Vertex 80 from Bruker). Additional details about this smog chamber are given elsewhere (Doussin et al., 1997;
Duncianu et al., 2017).

186   The relative rate technique was used to determine the rate constant for the OH-oxidation of the carbonyl nitrates
with methanol as reference compound. We used the IUPAC recommended value $k_{(methanol+OH)} = (9.0 \pm 1.8) \times$
188   10^{-13} cm^3 molecule^{-1} s^{-1} (http://www.iupac-kinetic.ch.cam.ac.uk/). Hydroxyl radicals were generated by
photolyzing isopropyl nitrite. Initial mixing ratios of reactants (carbonyl nitrate, isopropyl nitrite, methanol and
190   NO) were in the ppm range. As previously described, the carbonyl nitrate was introduced into the chamber by
connecting the bulb to the chamber and by slightly heating and flushing it with N_2. NO was added to the mixture
192   in order to enhance the formation of OH radicals by reaction with HO_2 radicals which are formed by isopropyl
nitrite photolysis. All experiments were conducted during a 1 h period of continuous irradiation.

194   Prior to the experiments, it was verified that photolysis and wall losses of the studied compounds were negligible
under our experimental conditions. This can be explained by the facts that i) the irradiation system of CSA
196   chamber emits photons at significantly higher wavelengths than the one of CESAM chamber, and ii) the walls of
the chamber are made of Pyrex which is more chemically inert than stainless steel. It was therefore assumed that
198   reaction with OH is the only fate of both, the studied compound (nitrate) and the reference compound (methanol)
and that neither of these compounds is reformed at any stage during the experiment. Based on these hypotheses,
200   it can be shown that (Atkinson, 1986):

$$ln \frac{[nitrate]_0}{[nitrate]_t} = \frac{k_{nitrate}}{k_{methanol}} \times \frac{[methanol]_0}{[methanol]_t} \qquad \text{(Eq. 3)}$$

202   where [nitrate]$_0$ and [methanol]$_0$, and [nitrate]$_t$ and [methanol]$_t$ stand for the concentration of the carbonyl nitrate
and the reference compound at times 0 and t, respectively. The plot ln([nitrate]$_0$/[nitrate]$_t$) *vs.*
204   ln([methanol]$_0$/[methanol]$_t$) is linear with a slope equal to $k_{nitrate}$/$k_{methanol}$ and an intercept of zero. The uncertainty
on $k_{nitrate}$ was calculated by adding the relative uncertainty corresponding to the statistical error on the linear
206   regression (2σ) and the error on the reference rate constant (here 20 % for methanol).

2.4 Chemicals and gases

208   Dry synthetic air was generated using N_2 (from liquid nitrogen evaporation, >99.995% pure, <5 ppm H_2O, Linde
Gas) and O_2 (quality N45, >99.995% pure, <5 ppm H_2O, Air Liquide). Chemicals obtained from commercial
210   sources are: NO (quality N20, >99% Air Liquide), NO_2 (quality N20, >99% Air Liquide), 4-hydroxy-2-butanone
(95% Aldich), 5-hydroxy-2-pentanone (95% Aldich), cyclohexane (VWR), methanol (J.T. Baker), H_2SO_4 (95%
212   VWR), $NaNO_2$ (≥99 Prolabo), isopropanol (VWR).

3 Results and discussion

3.1 Photolysis of carbonyl nitrates
214

Photolyses of 4-nitrooxy-2-butanone and 5-nitrooxy-2-pentanone were investigated for the first time. Figure 1
216   presents the kinetic plots obtained for the two compounds, where ln[nitrate] was plotted as a function of time. A

significant decrease was observed for both compounds during the dark period, before and after irradiation, suggesting that they adsorb or decompose on the walls. Photolysis frequencies were thus calculated as the difference between the decay rates in the dark and the one under irradiation (see section 2.2). Results obtained for both compounds and for all experiments are given in Table 1. For 4-nitrooxy-2-butanone, photolysis frequencies are in good agreement despite the fact that decay rates in the dark differ from an experiment to another. For 5-nitrooxy-2-butanone, it can be seen that the decay rate in the dark before irradiation is significantly higher than the one after (in particular for experiments 3 and 4), suggesting that wall losses may decrease with time due to a passivation of the walls. Despite this, comparison of the three experiments showed good agreement. For CESAM irradiation conditions, the photolysis rates are $(1.3 \pm 0.2) \times 10^{-5}$ s^{-1} for 4-nitrooxy-2-butanone and $(0.7 \pm 0.2) \times 10^{-5}$ s^{-1} for 5-nitrooxy-2-pentanone. These results have been compared in Table 2 to those we obtained in a previous study (Suarez-Bertoa et al., 2012) for 3-nitrooxy-2-propanone, 3-nitrooxy-2-butanone and 3-methyl-3-nitrooxy-2-butanone using the same experimental conditions and methodology. Experimental photolysis frequencies have also been compared to those calculated using cross sections published in the literature and by assuming a quantum yield equal to unity. The intensity of the actinic flux in CESAM chamber was determined by combining measurement of the spectrum of the lamps with a spectroradiometer and determination of J_{NO2} by chemical actinometry (see section 2.2). For 3-nitrooxy-2-propanone and 3-nitrooxy-2-butanone, cross sections were taken from Barnes et al. (1993). For 4-nitrooxy-2-butanone and 5-nitrooxy-2-pentanone, for which no data have been provided in the literature, cross sections were estimated using those for corresponding monofunctional species and by applying the enhancement factor (r_{nk}) obtained for 3-nitrooxy-2-propanone (Müller et al., 2014):

$$r_{nk} = \frac{s_{nk}}{s_n + s_k} \qquad\qquad\qquad\qquad\qquad \text{(Eq.4)}$$

Where s_{nk}, s_n and s_k are the absorption cross sections of the keto nitrate, the alkyl nitrate and the ketone, respectively. For 4-nitrooxy-2-butanone, cross sections of 2-butanone and 1-butyl nitrate were taken from IUPAC, 2006. For 5-nitroxy-2-pentanone, cross sections of 2-pentanone (http://satellite.mpic.de/spectral_atlas) and 1-pentyl nitrate (Clemitshaw et al., 1997) were used. From these results, it can be observed that the experimental photolysis frequencies (J_{exp}) obtained for 3-nitrooxy-2-propanone and 4-nitrooxy-2-butanone are very close and can be considered as equal within uncertainties. This suggests that the strong enhancement in the cross sections induced by the interaction between the two functional groups, which has been observed for α-nitrooxy ketones, also exists with the same amplitude for β-nitrooxy ketones. This is confirmed by the fact the experimental value for 4-nitrooxy-2-butanone is in very good agreement with the calculated value, obtained by assuming that the enhancement factor is the same as the one for 3-nitrooxy-2-propanone. This effect, nonetheless, seems to fade away when the two functions are one carbon further away: The experimental photolysis frequency obtained for 5-nitrooxy-2-pentanone is indeed significantly lower than those for 3-nitrooxy-2-propanone and 4-nitrooxy-2-butanone. It is also much lower than the J value calculated by assuming the same enhancement factor as for 3-nitrooxy-2-propanone. This result suggests that the enhancement is significantly reduced for γ-nitrooxy ketones even if it is probably not totally absent. This can easily be explained by the fact that the inductive effect of the nitrate group is expected to decrease when the distance between the functional groups increases. Finally, by comparing results for 3-nitrooxy-2-propanone, 3-nitrooxy-2-butanone and 3-methyl-3-nitrooxy-2-butanone, it can be observed that photolysis frequencies increase with the substitution

256   of the alkyl chain. From these kinetic data, it can be concluded that photolysis frequencies of α- and β-nitrooxy

ketones are much higher than those obtained when considering the sum of the photolysis frequencies for

258   monofunctional species.

Products formed by the photolysis of the carbonyl nitrates were investigated by FTIR spectrometry. For both

260   compounds, only PAN was detected. To calculate its formation yield, concentration of PAN was plotted as a

function of $-\Delta[\text{nitrate}]_{\text{photolysis}}$, i.e., the carbonyl nitrate loss rate due to photolysis. This one was calculated by

262   subtracting the loss rate measured during the dark period before the photolysis to the one measured during the

photolysis. Because the yield was calculated as the initial slope of the plot, it was considered that the dark period

264   before irradiation was more representative than the one after. The uncertainty on the yield was calculated by

taking into account the uncertainties on the infrared absorption cross sections of PAN (10%) and carbonyl

266   nitrates (10%) as well as the uncertainty on J (see table 1). For 5-nitrooxy-2-pentanone, this uncertainty is quite

large because the photolysis rate is relatively slow in comparison to loss to the reactor walls. PAN formation

268   yields obtained for both compounds are given in Table 1.

For 4-nitrooxy-2-butanone, PAN is formed with a yield equal to unity. Its formation can be explained by the

270   dissociation of the C(O)-C bond as shown in Scheme 1. This pathway also leads to the formation of the alkyl

radical $^{\bullet}CH_2\text{-}CH_2ONO_2$ which reacts with O_2 to form the corresponding peroxy radical, this latter evolving to the

272   formation of the alkoxy by reaction with NO. Two pathways have been considered for the evolution of the

alkoxy radical: i) the decomposition which may lead to the formation of NO_2 and two molecules of HCHO and

274   ii) the reaction with O_2 which produces nitrooxy ethanal, also called ethanal nitrate ($CH_2(ONO_2)\text{-}CH(O)$). None

of these two products have been detected by FTIR. However, absorption bands of ethanal nitrate are expected to

276   be very similar to those of the reactant and it may thus be difficult to distinguish them. In addition, ethanal

nitrate is expected to photodissociate much faster than the keto nitrate. The other photodissociation pathway is

278   the cleavage of the $O\text{-}NO_2$ bond. It leads to the formation of the radical $CH_3C(O)CH_2CH_2O^{\bullet}$ which is expected

to react with O_2 to form a dicarbonyl product. This product was not observed and this is in good agreement with

280   the formation of PAN with a yield equal to unity by the other photodissociation pathway. It should be noticed

that PAN has been detected as a primary product suggesting that its formation via the photolysis of the

282   dicarbonyl product is not expected. In our experiments, it was not possible to measure NO_2 formation yield

because large amounts of NO_2 (hundreds ppb) were introduced with the carbonyl nitrate (probably due to its

284   decomposition during the injection).

As discussed above, since the enhancement in the cross sections is larger at the higher wavelengths, where

286   absorption by the nitrate chromophore is very small, it was proposed by Müller et al. (2014) that the absorption

by the carbonyl chromophore is enhanced due to the neighboring nitrate group. The authors also suggest that the

288   photodissociation proceeds by a dissociation of the weak $O\text{-}NO_2$ bond, i.e. that a photon absorption by one

chromophore (carbonyl group) causes dissociation in another part of the molecule (nitro group). This is not in

290   line with what we observed in our study. From our experiments, we conclude that the photolysis of 4-nitrooxy-2-

butanone proceeds mainly by a dissociation of the C(O)-C bond. In the former study on the photolysis of 3-

292   nitrooxy-2-propanone, 3-nitrooxy-2-butanone and 3-methyl-3-nitrooxy-2-butanone (Suarez-Bertoa et al., 2012),

PAN and carbonyl compounds (respectively, formaldehyde, acetaldehyde and acetone) were detected as major

294 products. However, branching ratio of the two pathways (dissociation of O-NO$_2$ and C(O)-C bonds) could not be determined as the formation of these products, in particular PAN, can be explained by the two pathways.

296 For 5-nitrooxy-2-pentanone, formation yield of PAN has been observed to be much lower: 0.16 ± 0.08. As for 4-nitrooxy-2-butanone, its formation can be explained by the dissociation of the C(O)-C bond (see Scheme 3). This

298 result suggests that both dissociation pathways may occur and that O-NO$_2$ dissociation could be the major one. However, this was not confirmed by the detection of the dicarbonyl compound (2-oxo-pentanal) which is

300 expected to be formed by this pathway. Despite the fact that no standard was available for this compound, no characteristic band was observed in the residual spectrum (after subtraction of reactants and PAN spectra).

302 Because the photolysis rate of 5-nitrooxy-2-pentanone is very low, we suspect that the concentration of this product is below the detection limit. Nevertheless, the low PAN yield is a strong indication that O-NO$_2$

304 dissociation may be the major pathway, contrary to what has been observed for 4-nitrooxy-2-butanone. This should be considered in the light of the low enhancement of absorption cross sections which has been assumed

306 for this compound. Hence, in the case of γ-nitrooxy ketones, the enhancement of the absorption by the carbonyl chromophore seems to significantly decrease, leading to a lower branching ratio of the C(O)-C bond

308 dissociation.

3.2 OH-oxidation of carbonyl nitrates

310 Rate constants of the OH-oxidation have been measured for 4-nitrooxy-2-butanone and 5-nitrooxy-2-pentanone. Prior to the experiments, it was checked that the carbonyl nitrates do not photolyse nor decompose/adsorb on the

312 walls of the chamber. Figure 2 represents the kinetic plots obtained for the two carbonyl nitrates. For each compound, several independent kinetic experiments were performed and data were combined to provide the

314 $k_{ketonitrate}/k_{methanol}$ for each compound (see Figure 3). In order to limit errors in the quantification of reactants due to the possible formation of carbonyl nitrates as products, only the very beginning of the experiments was taken

316 into account for the kinetic plots. This explains the small number of experimental points. The obtained rate constants are given in Table 3. These data are, to our knowledge, the first determinations of the rate constants for

318 the reaction of OH with these two carbonyl nitrates. From these data, it can be concluded that 4-nitrooxy-2-butanone and 5-nitrooxy-5-pentanone have similar reactivity towards OH radicals with rate constants equal to

320 $(2.9 \pm 1.0) \times 10^{-12}$ and $(3.3 \pm 0.9) \times 10^{-12}$ cm^3 molecule^{-1} s^{-1}, respectively.

Rate constants provided in this study, as well as those previously reported for a series of α-nitrooxy-ketones

322 (Suarez-Bertoa et al., 2012) have been compared to those estimated using structure-activity relationships (SARs) in Table 4. Different SARs have been evaluated: i) the one developed by Kwok and Atkinson (1995) with

324 updated factors F(-ONO$_2$) = 0.14 and F(-C-ONO$_2$) = 0.28 from Bedjanian et al. (2018); ii) the one developed by Kwok and Atkinson (1995) with updated factors F(-ONO$_2$) = 0.8 and F(-C-ONO$_2$) = 0.1 from Suarez-Bertoa et

326 al. (2012); iii) the one developed by Neeb (2000) which proposes a different type of parametrization and has been observed to be particularly accurate for oxygenated species; and iv) the one developed by Jenkin et al.

328 (2018) which proposes a parametrization very similar to the one from Kwok and Atkinson (1995) and Bedjanian et al. (2018). The rate constant for 5-nitrooxy-2-pentanone is reasonably well reproduced by all SARs (within a

330 factor of 2). For 4-nitrooxy-2-butanone, only the parametrization provided by Suarez-Bertoa et al. (2012) succeeds in reproducing the experimental value. This can be explained by the fact that this parametrization has

332 been optimized for carbonyl nitrates while the others have been developed using the entire dataset for

compounds containing a nitrate group (-ONO_2) (Jenkin et al., 2018) or using the dataset for alkyl nitrates

334 (Bedjanian et al., 2018). The main difference between these parametrizations is that in Suarez-Bertoa et al.

(2012), the factor F(-ONO_2) is much less deactivating than for the others. This could result from electronic

336 interactions between the two functional groups. However, Suarez-Bertoa et al. (2012) noticed that their

parametrization gives poor results for alkyl nitrates, suggesting that a specific parametrization has to be used for

338 multifunctional species. This also suggests that the principle of SARs based on the group additivity method may

not be suitable for multifunctional molecules.

340 From these experiments, several oxidation products have been detected: HCHO, PAN and methylglyoxal for 4-

nitrooxy-2-butanone, and HCHO, PAN and 3-nitrooxy-propanal for 5-nitrooxy-2-pentanone. However, their

342 quantification was highly uncertain because the infrared spectra were complex due to the presence of methanol,

isopropyl nitrite, impurities (in particular acetic acid) and their oxidation products. Dedicated mechanistic

344 experiments should now/in the near future be performed using HONO as OH source in order to simplify the

chemical mixture.

346 **3.3 Atmospheric implications**

Atmospheric lifetimes of the investigated compounds are presented in Table 5. The photolysis rates were

348 estimated for typical tropospheric irradiation conditions corresponding to the 1st July at noon and at 40° latitude

North. Thanks to the realism of the irradiation in CESAM chamber, they were calculated by applying a factor 4.7

350 to the photolysis frequencies measured in the chamber (see section 2.2). They are: $(6.1 \pm 0.9) \times 10^{-5}$ s^{-1} for 4-

nitrooxy-2-butanone and $(3.3 \pm 0.9) \times 10^{-5}$ s^{-1} for 5-nitrooxy-2-pentanone. Under these irradiation conditions,

352 lifetimes (τ_{hv} = 1/J) were found to be 4 and 8 hours, respectively. For OH-oxidation, lifetimes (τ_{OH}=

$(1/(k_{OH}[OH]))$ were calculated using typical OH concentrations of 2×10^6 molecule cm^{-3} (Atkinson and Arey,

354 2003). They are both equal to approximatively two days. Hence, it appears that for 4-nitrooxy-2-butanone and

for 5-nitrooxy-2-pentanone, photolysis is a more efficient sink than oxidation by OH radicals. An identical

356 conclusion was obtained for α-nitrooxy carbonyls (Suarez-Bertoa et al., 2012; Barnes et al., 1993; Zhu et al.,

1991). However, OH-initiated oxidation is not negligible, especially under polluted conditions where OH

358 concentrations can be higher than 1×10^7 molecule cm^{-3}.

In order to evaluate the impact of these carbonyl nitrates on the nitrogen budget and the transport of NOx, it is

360 crucial to determine whether their atmospheric sinks, here mainly photolysis, release NO_2 or not. For 4-nitrooxy-

2-butanone, we observed that the photolysis proceeds mainly by a dissociation of the C(O)-C bond which does

362 not necessarily lead to the release of NO_2 (see Scheme 2). In our experimental conditions (i.e., with high NO_2

mixing ratios), this pathway leads to the formation of PAN which was detected with a yield equal to unity.

364 Under more realistic NO/NO_2 ratio, this reaction may also produce HCHO and CO_2. The co-products of PAN,

which could not be detected in our study, are expected to be formaldehyde + NO_2 or ethanal nitrate. One NO_2

366 molecule is hence released in the first hypothesis. Ethanal nitrate may react and undergo photolysis even faster

than nitrooxy ketones and may thus lead to NO_2 release quite rapidly. However, as data on the reactivity of

368 ethanal nitrate are not available in the literature, one cannot provide a definite conclusion. In the case of 5-

nitrooxy-2-pentanone, the dissociation of the C(O)-C bond has been observed to be a minor pathway suggesting

370 that the major one, which was not directly observed here, is the O-NO$_2$ dissociation. This process certainly leads to the release of NO$_2$.

4 Conclusions

This work represents the first study on the atmospheric reactivity of 4-nitrooxy-2-butanone and 5-nitrooxy-2-pentanone. Thanks to experiments in simulation chambers, photolysis frequencies and rate constants of the OH-oxidation were measured for the first time. From these results, it is concluded that, similarly to α-nitrooxy ketones, β-nitrooxy ketones have enhanced UV absorption cross sections and quantum yields equal or close to unity, making photolysis a very efficient sink for these compounds. Results obtained for 5-nitrooxy-2-pentanone which is a γ-nitrooxy ketone, suggest a lower enhancement of cross sections leading to slightly longer atmospheric lifetimes. This can easily be explained by the increasing distance between the two chromophore groups. Some photolysis products were also detected allowing estimating the branching ratio between the two possible pathways, i.e., the dissociation of the C(O)-C bond and the one of the O-NO$_2$ bond. For 4-nitrooxy-2-butanone, we conclude that the photolysis proceeds mainly by a dissociation of the C(O)-C bond which does not necessarily lead to the release of NO$_2$. In the case of 5-nitrooxy-2-pentanone, our results suggest that the dissociation of the O-NO$_2$ bond is the major pathway. Reactivity of 4-nitrooxy-2-butanone and 5-nitrooxy-2-pentanone with OH radicals was also investigated. Both compounds have similar reactivity towards OH radicals leading to lifetimes of approximatively two days. Experimental rate constants are in good agreement with those estimated by the SAR proposed by Kwok and Atkinson (1995) when using the parametrization proposed by Suarez-Bertoa et al. (2012) for carbonyl nitrates. However, this specific parametrization does not allow reproducing experimental data for monofunctional alkyl nitrates, suggesting that specific parametrization should be used for multifunctional species. Finally, these compounds are expected to be removed from the atmosphere fairly rapidly and to act as (only) temporary reservoirs of NOx. If formed during the night, they could however contribute to longer range transport of NOx.

References

410   Atkinson, R., and Arey, J.: Gas-phase tropospheric chemistry of biogenic volatile organic compounds: a review, Atmos. Environ., 37, 197-219, 2003.

412   Barnes, I., Becker, K. H., and Zhu, T.: Near UV absorption spectra and photolysis products of difunctional organic nitrates: possible importance as NOx Reservoirs, J. Atmos. Chem., 17, 353-373,

414   1993.

        Bean, J. K., and Hildebrand Ruiz, L.: Hydrolysis and gas-particle partitioning of organic nitrates formed

416   from the oxidation of α-pinene in environmental chamber experiments, Atmos. Chem. Phys. 15, 20629-20653, 2015.

418   Beaver, M. R., St Clair, J. M., Paulot, F., Spencer, K. M., Crounse, J. D., LaFranchi, B. W., Min, K. E., Pusede, S. E., Wooldridge, P. J., Schade, G. W., Park, C., Cohen, R. C., and Wennberg, P. O.:

420   Importance of biogenic precursors to the budget of organic nitrates: observations of multifunctional organic nitrates by CIMS and TD-LIF during BEARPEX 2009, Atmos. Chem. Phys., 12, 5773-5785,

422   2012.

        Bedjanian, Y., Morin, J., and Romanias, M. N.: Reactions of OH radicals with 2-methyl-1-butyl,

424   neopentyl and 1-hexyl nitrates. Structure-activity relationship for gas-phase reactions of OH with alkyl nitrates: An update, Atmos. Environ., 180, 167-172, 2018.

426   Clemitshaw, K. C., Williams, J., Rattigan, O. V., Shallcross, D. E., Law, K. S., and Cox, R. A.: Gas-phase ultraviolet absorption cross-sections and atmospheric lifetimes of several C2-C5 alkyl nitrates, J.

428   Photochem. Photobiol. A, 102, 117-126, 1997.

        Doussin, J. F., Ritz, D., Durand-Jolibois, R., Monod, A., and Carlier, P.: Design of an environmental

430   chamber for the study of atmospheric chemistry: New developments in the analytical device, Analusis, 25, 236-242, 1997.

432   Duncianu, M., David, M., Kartigueyane, S., Cirtog, M., Doussin, J. F., and Picquet-Varrault, B.: Measurement of alkyl and multifunctional organic nitrates by Proton Transfer Reaction Mass

434   Spectrometry, Atmos. Meas. Tech., 10, 1445-1463, 2017.

        Finlayson-Pitts, B. J., and Pitts Jr., J. N.: Chemistry of the Upper and Lower Atmosphere, Academic

436   Press, San Diego, 2000.

        Horowitz, L. W., Fiore, A. M., Milly, G. P., Cohen, R. C., Perring, A., Wooldridge, P. J., Hess, P. G.,

438   Emmons, L. K., and Lamarque, J.-F.: Observational constraints on the chemistry of isoprene nitrates over the eastern United States, J. Geophys. Res., 112, D12S08, 2007.

440   Ito, A., Sillman, S., and Penner, J. E.: Effects of additional nonmethane volatile organic compounds, organic nitrates, and direct emissions of oxygenated organic species on global tropospheric chemistry,

442   Journal of Geophysical Research-Atmospheres, 112, 10.1029/2005jd006556, 2007.

444   Jenkin, M. E., Valorso, R., Aumont, B., Rickard, A. R., and Wallington, T. J.: Estimation of rate coefficients and branching ratios for gas-phase reactions of OH with aliphatic organic compounds for use in automated mechanism construction, Atmos. Chem. Phys., 18, 9297-9328, 10.5194/acp-18-9297-2018, 446   2018.

Kames, J., Schurath, U., Flocke, F., and Volz-Thomas, A.: Preparation of organic nitrates from alcohols 448   and N_2O_5 for species identification in atmospheric samples, J. Atmos. Chem., 16, 349-359, 1993.

Kwok, E. S. C., and Atkinson, R.: Estimation of Hydroxyl Radical Reaction Rate Constants for Gas-450   Phase Organic Compounds using a Structure-Reactivity Relationship: an update, Atmos. Environ., 29, 1685-1695, 1995.

452   Mao, J. Q., Paulot, F., Jacob, D. J., Cohen, R. C., Crounse, J. D., Wennberg, P. O., Keller, C. A., Hudman, R. C., Barkley, M. P., and Horowitz, L. W.: Ozone and organic nitrates over the eastern United 454   States: Sensitivity to isoprene chemistry, Journal of Geophysical Research-Atmospheres, 118, 11256-11268, 10.1002/jgrd.50817, 2013.

456   Muller, J. F., Peeters, J., and Stavrakou, T.: Fast photolysis of carbonyl nitrates from isoprene, Atmos. Chem. Phys., 14, 2497-2508, 10.5194/acp-14-2497-2014, 2014.

458   Neeb, P.: Structure-Reactivity Based Estimation of the Rate Constants for Hydroxyl Radical Reactions with Hydrocarbons, J. Atmos. Chem., 35, 295-315, 2000.

460   Ng, N. L., Brown, S. S., Archibald, A. T., Atlas, E., Cohen, R. C., Crowley, J. N., Day, D. A., Donahue, N. M., Fry, J. L., Fuchs, H., Griffin, R. J., Guzman, M. I., Herrmann, H., Hodzic, A., Iinuma, Y., 462   Jimenez, J. L., Kiendler-Scharr, A., Lee, B. H., Luecken, D. J., Mao, J. Q., McLaren, R., Mutzel, A., Osthoff, H. D., Ouyang, B., Picquet-Varrault, B., Platt, U., Pye, H. O. T., Rudich, Y., Schwantes, R. H., 464   Shiraiwa, M., Stutz, J., Thornton, J. A., Tilgner, A., Williams, B. J., and Zaveri, R. A.: Nitrate radicals and biogenic volatile organic compounds: oxidation, mechanisms, and organic aerosol, Atmos. Chem. 466   Phys., 17, 2103-2162, 10.5194/acp-17-2103-2017, 2017.

Paulot, F., Crounse, J. D., Kjaergaard, H. G., Kroll, J. H., Seinfeld, J. H., and Wennberg, P. O.: Isoprene 468   photooxidation: new insights into the production of acids and organic nitrates, Atmos. Chem. Phys., 9, 1479-1501, 10.5194/acp-9-1479-2009, 2009.

470   Perring, A. E., Bertram, T. H., Farmer, D. K., Wooldridge, P. J., Dibb, J., Blake, N. J., Blake, D. R., Singh, H. B., Fuelberg, H., Diskin, G., Sachse, G., and Cohen, R. C.: The production and persistence of 472   Sigma $RONO_2$ in the Mexico City plume, Atmos. Chem. Phys., 10, 7215-7229, 10.5194/acp-10-7215-2010, 2010.

474   Perring, A. E., Pusede, S. E., and Cohen, R. C.: An Observational Perspective on the Atmospheric Impacts of Alkyl and Multifunctional Nitrates on Ozone and Secondary Organic Aerosol, Chemical 476   Reviews, 113, 5848-5870, 10.1021/cr300520x, 2013.

Rindelaub, J. D., McAvey, K. M., and Shepson, P. B.: The photochemical production of organic nitrates 478   from alpha-pinene and loss via acid-dependent particle phase hydrolysis, Atmos. Environ., 100, 193-201, 10.1016/j.atmosenv.2014.10.010, 2015.

480   Roberts, J. M.: The Atmospheric Chemistry of organic Nitrates, Atmos. Environ., 24A, 243-287, 1990.

482   Scarfogliero, M., Picquet-Varrault, B., Salce, J., Durand-Jolibois, R., and Doussin, J.-F.: Kinetic and Mechanistic Study of the Gas-Phase Reactions of a Series of Vinyl Ethers with the Nitrate Radical, J. Phys. Chem. A, 110, 11074-11081, 2006.

484   Squire, O. J., Archibald, A. T., Griffiths, P. T., Jenkin, M. E., Smith, D., and Pyle, J. A.: Influence of isoprene chemical mechanism on modelled changes in tropospheric ozone due to climate and land use 486   over the 21st century, Atmos. Chem. Phys., 15, 5123-5143, 10.5194/acp-15-5123-2015, 2015.

    Suarez-Bertoa, R., Picquet-Varrault, B., Tamas, W., Pangui, E., and Doussin, J. F.: Atmospheric Fate of a 488   Series of Carbonyl Nitrates: Photolysis Frequencies and OH-Oxidation Rate Constants, Environ. Sci. Technol., 46, 12502-12509, 10.1021/es302613x, 2012.

490   Taylor, W. D., Allston, T. D., Moscato, M. J., Fazenkas, G. B., Koslowski, R., and Takacs, G. A.: Atmospheric Photodissociation lifetimes for nitromethane, methyl nitrite, and methyl nitrate., Int. J. 492   Chem. Kinet., 12, 231-240, 1980.

    Turberg, M. P., Giolando, D. M., Tilt, C., Soper, T., Mason, S., Davies, M., Klingensmith, P., and 494   Takacs, G. A.: Atmospheric Photochemistry of Alkyl Nitrates, J. Photochem. Photobiol. A-Chem., 51, 281-292, 1990.

496   Wang, J., Doussin, J. F., Perrier, S., Perraudin, E., Katrib, Y., Pangui, E., and Picquet-Varrault, B.: Design of a new multi-phase experimental simulation chamber for atmospheric photosmog, aerosol and 498   cloud chemistry research, Atmospheric Measurement Techniques, 4, 2465-2494, 10.5194/amt-4-2465-2011, 2011.

500   Xiong, F. L. Z., Borca, C. H., Slipchenko, L. V., and Shepson, P. B.: Photochemical degradation of isoprene-derived 4,1-nitrooxy enal, Atmos. Chem. Phys., 16, 5595-5610, 10.5194/acp-16-5595-2016, 502   2016.

    Zhu, T., Barnes, I., and Becker, K. H.: Relative-rate study of the gas-phase reaction of hydroxy radicals 504   with difunctional organic nitrates at 298K and atmospheric pressure, J. Atmos. Chem., 13, 301-311, 1991.

506

508

Figure, scheme and table captions

Scheme 1. Photolysis pathways of 4-nitrooxy-2-butanone

Scheme 2. Photolysis pathways of 5-nitrooxy-2-pentanone

Figure 1. Kinetic plots for *(a)* the photolysis of 4-nitrooxy-2-butanone (experiment 2) and *(b)* the photolysis of 5-nitrooxy-2-pentanone (experiment 5). Red lines correspond to linear regressions.

Figure 2. Kinetic plots for the oxidation by OH radicals of 4-nitrooxy-2-butanone and 5-nitrooxy-2-pentanone. For 5-nitrooxy-2-pentanone, data have been shifted by 0.2 in y axis.

Table 1. Photolysis rate and PAN yield for 4-nitrooxy-2-butanone and 5-nitrooxy-2-pentanone.

Table 2. Comparison of experimental photolysis rates of carbonyl nitrates with calculated ones obtained for CESAM irradiation conditions.

**Table 3.** Rate constants for the OH-oxidation of 4-nitrooxy-2-butanone and 5-nitrooxy-2-pentanone

Table 4. Comparison of experimental rate constants for the OH-oxidation of carbonyl nitrates with those estimated by SARs

Table 5. Atmospheric lifetimes of carbonyl nitrates towards photolysis and reaction with OH radicals
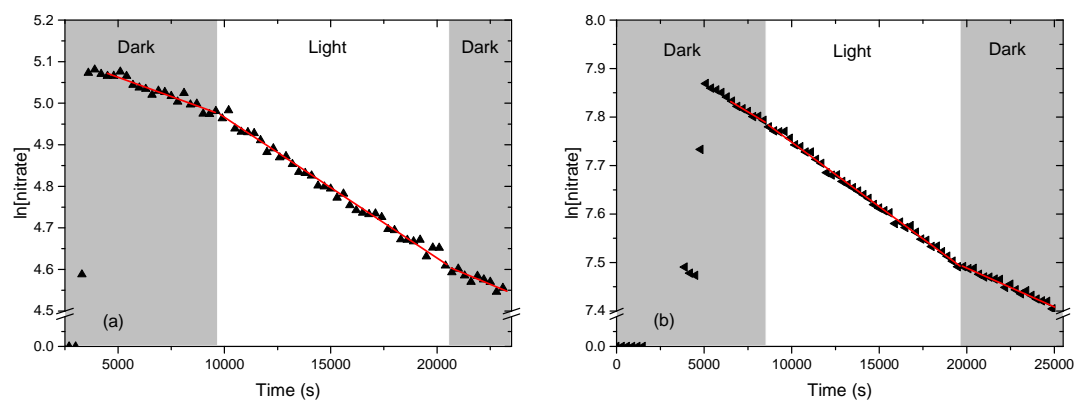
526
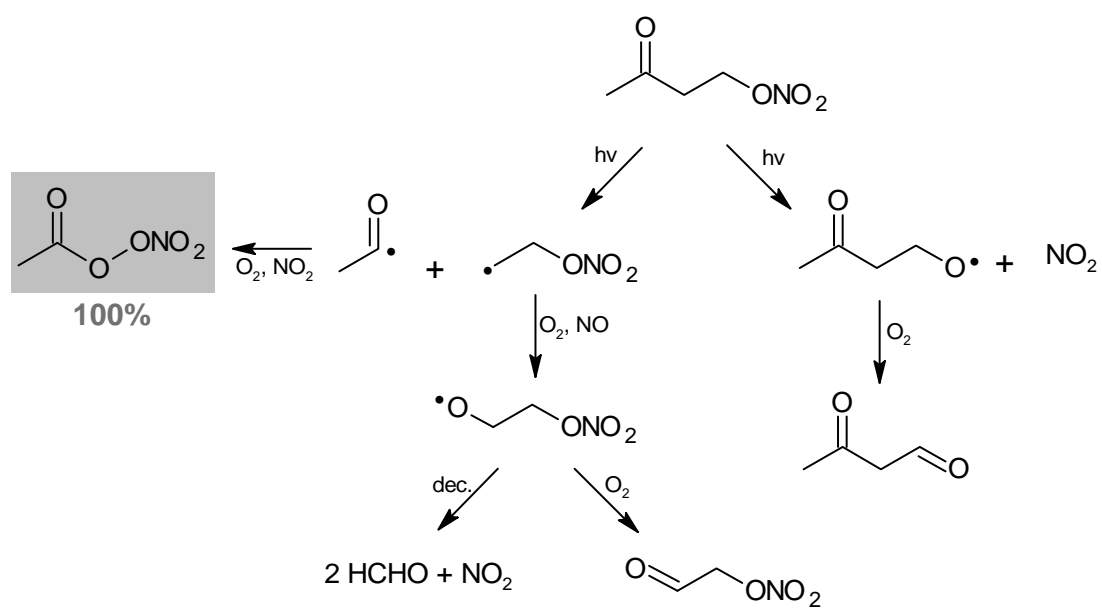
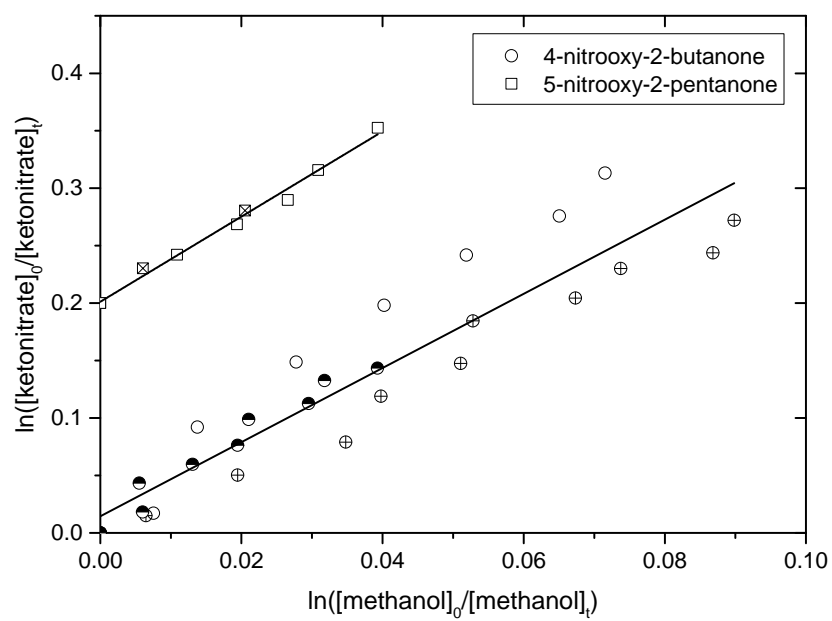
528   **Scheme 1.**
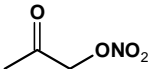
530

Scheme 2.

532

Figure 1.

542

Figure 2.

544
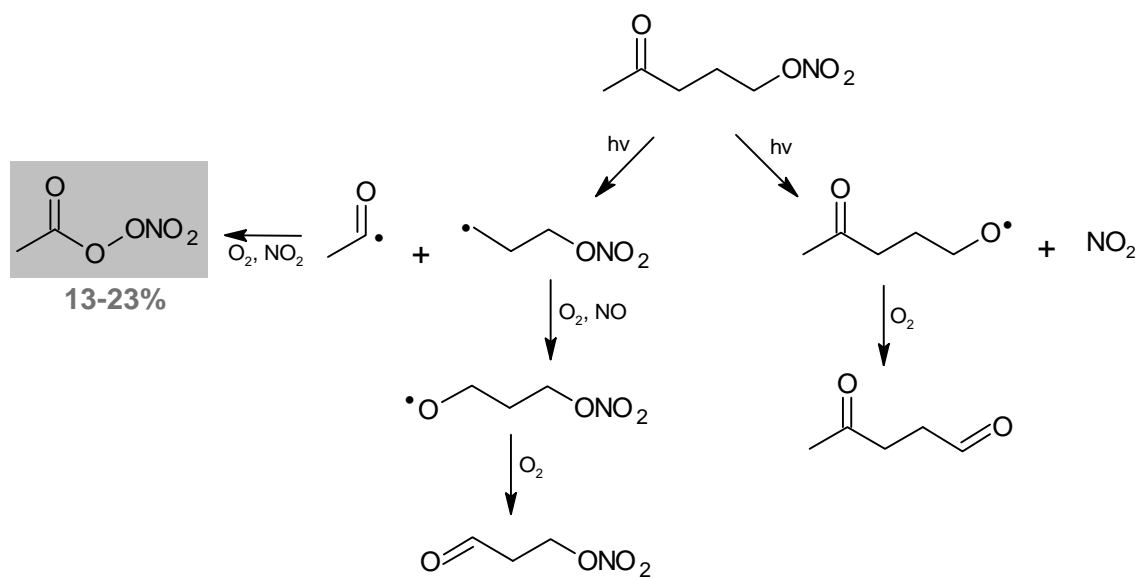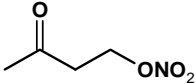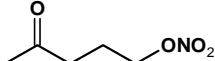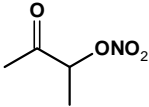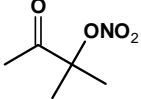
Table 1.

Compound	Experim.	k_{before} [a] ($\times 10^{-5}$ s^{-1})	k_{after} [b] ($\times 10^{-5}$ s^{-1})	(k+J) [c] ($\times 10^{-5}$ s^{-1})	J [d] ($\times 10^{-5}$ s^{-1})	PAN yield (%)
4-nitrooxy-2-butanone	1	0.8 ± 0.1	-	2.1 ± 0.1	1.3 ± 0.2	100 ± 35
	2	1.9 ± 0.2	2.1 ± 0.1	3.3 ± 0.1	1.3 ± 0.3	100 ± 40
	Average				**1.3 ± 0.2**	**100 ± 30**
5-nitrooxy-2-pentanone	3	2.0 ± 0.2	1.1 ± 0.2	2.3 ± 0.1	0.7 ± 0.4	13 ± 9
	4	1.9 ± 0.2	1.1 ± 0.1	2.2 ± 0.1	0.7 ± 0.4	13 ± 9
	5	2.1 ± 0.2	1.6 ± 0.2	2.7 ± 0.1	0.8 ± 0.3	23 ± 13
	Average				**0.7 ± 0.2**	**16 ± 8**

[a, b] dark decay due to wall loss, before and after irradiation; [c] decay during irradiation period;

546 [d] photolysis rate;

548

550

552 **Table 2.**

Compound	J_{exp} ($\times 10^{-5}$ s^{-1})	J_{calc} ($\times 10^{-5}$ s^{-1}) (ϕ=1)
3-nitrooxy-2-propanone	1.5 ± 0.1 (Suarez-Bertoa et al., 2012)	1.4[b]
4-nitrooxy-2-butanone	1.3 ± 0.2 (This work)	1.6[a]
5-nitrooxy-2-pentanone	0.7 ± 0.2 (This work)	1.8[a]
3-nitrooxy-2-butanone	1.8 ± 0.1 (Suarez-Bertoa et al., 2012)	2.2[b]
3-methyl-3-nitrooxy-2-butanone	2.31 ± 0.05 (Suarez-Bertoa et al., 2012)	ND

[a] calculated with estimated cross sections (see text); [b] calculated with experimental cross sections

554 from literature;

Table 3.

Compound	$k_{nitrate}/k_{methanol}$	$k_{nitrate} \times 10^{-12}$ (cm^3 molecule^{-1} s^{-1})
4-nitrooxy-2-butanone	3.25 ± 0.47	2.9 ± 1.0
5-nitrooxy-2-pentanone	3.70 ± 0.28	3.3 ± 0.9

556 **Table 4.**

Compound	k_{exp} x 10^{-13}	k_{SAR} Atkinson/Bedjanian[a] x 10^{-13}	k_{SAR} Atkinson/Suarez[b] x 10^{-13}	$k_{SAR\ Neeb}$[c] x 10^{-13}	$k_{SAR\ Jenkin}$[d] x 10^{-13}
3-nitrooxy-2-propanone	6.7[5]	2.0	6.6	5.8	2.5
3-nitrooxy-2-butanone	10.1[e]	4.5	13.2	6.8	3.7
3-methyl-3nitrooxy-2-butanone	2.6[e]	4.0	2.1	2.4	4.3
4-nitrooxy-2-butanone	29[f]	8.1	30.9	8.7	8.1
5-nitrooxy-2-pentanone	33[f]	21.4	22.5	47.6	19.5

558 Rate constants are expressed in cm^3 molecule^{-1} s^{-1}; [a] SAR developed by Kwok and Atkinson (1995) with F(-ONO$_2$) and F(-C-ONO$_2$) from Bedjanian et al., 2018; [b] SAR developed by Kwok and Atkinson (1995) with F(-ONO$_2$) and F(-C-ONO$_2$) from Suarez-Bertoa et al., (2012) ; [c] SAR developed by Neeb (2000); [d] SAR developed
560 by Jenkin et al. (2018) ; [e] experimental data from Suarez-Bertoa et al. (2012); [f] This work.

Table 5.

Compound	$J \times 10^{-5}$ [a] (s^{-1})	$\tau_{h\nu}$ (hours)	$k_{OH} \times 10^{-12}$ (cm^3 molecule^{-1} s^{-1})	τ_{OH} [b] (hours)
4-nitrooxy-2-butanone	6.1 ± 0.9	4	2.9 ± 1.0	48
5-nitrooxy-2-pentanone	3.3 ± 0.9	8	3.3 ± 0.9	42

562   [a] photolysis frequencies estimated for a typical solar actinic flux (40°N, 1st July, noon) by applying a factor 4.7 to those measured in CESAM chamber (see section 2.2); [b] estimated for [OH] = 2×10^6 molecule cm^{-3}

564

566